Coherent Bayesian analysis of inspiral signals

2007 Class. Quantum Grav. 24 S607

(http://iopscience.iop.org/0264-9381/24/19/S23)

Class. Quantum Grav. **24** (2007) S607–S615 doi:10.1088/0264-9381/24/19/S23

Coherent Bayesian analysis of inspiral signals

Christian Röver[1], Renate Meyer[1], Gianluca M Guidi[2,3], Andrea Viceré[2,3] and Nelson Christensen[4]

[1] Department of Statistics, The University of Auckland, Auckland, New Zealand
[2] Università degli Studi di Urbino 'Carlo Bo', Urbino, Italy
[3] INFN, Sezione di Firenze, Florence, Italy
[4] Physics and Astronomy, Carleton College, Northfield, MN, USA

Received 31 March 2007, in final form 26 July 2007
Published 19 September 2007
Online at stacks.iop.org/CQG/24/S607

Abstract

In this paper we present a Bayesian parameter estimation method for the analysis of interferometric gravitational wave observations of an inspiral of binary compact objects using data recorded simultaneously by a network of several interferometers at different sites. We consider neutron star or black hole inspirals that are modeled to 3.5 post-Newtonian (PN) order in phase and 2.5 PN in amplitude. Inference is facilitated using Markov chain Monte Carlo (MCMC) methods that are adapted in order to efficiently explore the particular parameter space. Examples are shown to illustrate how and what information about the different parameters can be derived from the data. This study uses simulated signals and data with noise characteristics that are assumed to be defined by the LIGO and Virgo detectors operating at their design sensitivities. Nine parameters are estimated, including those associated with the binary system plus its location on the sky. We explain how this technique will be part of a detection pipeline for binary systems of compact objects with masses up to 20 $M_{\odot}$, including cases where the ratio of the individual masses can be extreme.

PACS numbers: 04.80.Nn, 02.70.Uu

1. Introduction

A worldwide network of interferometric gravitational wave detectors is now on-line. LIGO has reached its target sensitivity [1, 2] and Virgo is fast approaching theirs [3, 4]. GEO [5] and TAMA [6] are also participating in the search for gravitational waves. Compact binary systems will certainly produce gravitational waves [7] and they are likely to be one of the most promising sources.

The LIGO Scientific Collaboration (LSC) [8] and Virgo [9, 10] each have search pipelines for binary inspiral events, and studies have shown that these pipelines have equivalent detection

capabilities [11]. The LSC has conducted searches for binary neutron star inspirals [8, 12], primordial black hole binary coalescences in the galactic halo [13] and black hole binaries [14]. The LSC and TAMA have conducted a joint search for binary neutron star systems [15], and soon the LSC and Virgo will be conducting collaborative searches [11].

The purpose of a binary inspiral detection pipeline is to find a signal within the data. Once researchers suspect that a signal is present then parameter estimation techniques can be applied in order to produce estimates and summary statistics for the astrophysical parameters. Bayesian Markov chain Monte Carlo (MCMC) methods [16] are well suited for this problem, especially since it is possible to produce accurate predictions for the form of the signal. MCMC parameter estimation techniques have been developed for binary neutron star inspirals, as seen by a single interferometer [17]. In addition, MCMC methods have been developed for the coherent analysis of data from a worldwide network of interferometers [18].

A difficult detection scenario involves finding a signal produced by a binary system where the mass ratio between the two objects is large. In such a case, the signal will likely have its amplitude significantly modulated (as opposed to just a 'simple' chirp with monotonously increasing frequency and amplitude), and it will be necessary to use higher order post-Newtonian (PN) approximations. In this paper we present a description of our method for producing parameter estimates associated with a binary inspiral modeled to 3.5 post-Newtonain (PN) order in phase and 2.5 PN in amplitude [19, 21]. There are numerous goals that we wish to address with this version of our code. We employ new and more advanced MCMC methods, such as evolutionary MCMC [23]. The higher order PN templates will also allow for examination of signals where the amplitude is modulated, as may be the case with rather large ratios between the masses of the compact objects. Finally, we see this MCMC program as part of a larger detection pipeline for signals from binary inspirals with large mass ratios and individual masses going up to 20 $M_{\odot}$. We imagine, for example, using an existing detection pipeline [10] to generate a reasonable number of triggers; the MCMC would then analyze each of the triggers in detail. Once the MCMC has reached convergence, an estimate for the signal parameters would be produced. In this paper, we provide a description of the MCMC component of this detection pipeline.

2. Inference framework

2.1. The Bayesian approach

We follow a Bayesian approach in order to do inference on the inspiral signal's parameters, since this allows one to better address the questions of immediate interest in such a context. Other methods (e.g. matched-filtering methods) on the other hand usually follow a maximum-likelihood approach, which does not yield as satisfactorily interpretable results, and does not exploit the information available in the data to the same extent [24]. In a Bayesian setup, information about parameters is fomulated in terms of probability distributions on the parameter space. First, the pre-observational knowledge is expressed in the *prior distribution*, and inference is eventually done through the parameters' *posterior distribution* that is conditional on the observed data, and follows through the application of Bayes' theorem on the prior and the data model (likelihood). The parameters' posterior distribution then expresses the information about the parameters given the prior knowledge, the model and the data at hand [25–27].

2.2. MCMC methods

Once the Bayesian framework is set up, inference depends on evaluating the parameters' posterior distribution, which is given in terms of the (non-normalized) posterior density, in our case a function of nine parameters. Typically, one will be interested in figures such as posterior means, confidence bounds or marginal densities for individual parameters, which require integration of the posterior over the parameter space. This problem is commonly approached using Monte Carlo integration, i.e. by simulating random draws from the posterior distribution and then approximating the desired integrals by sample statistics (means by averages, etc). The most popular algorithms for this purpose are Markov chain Monte Carlo (MCMC) samplers that simulate a random walk through parameter space whose stationary distribution is the posterior distribution [16, 27].

Metropolis- (and related) MCMC algorithms also have nice optimization properties. In fact they happen to behave very similar to, e.g., a Nelder–Mead algorithm which is extended to a simulated annealing algorithm; on its random walk through parameter space it will always accept an 'uphill' step, and sometimes (randomly) a 'downhill' step aswell [28]. This property often comes in handy since the problem—as in our case—usually is not only to *sample* from the posterior, but also to first *find* the global posterior mode(s) within a complex posterior surface and among numerous minor modes. These convergence properties can also be enhanced through the implementation of the sampler, while care must be taken to maintain its ergodicity properties.

For our purposes we used a basic Metropolis sampler that we recently upgraded to an *evolutionary MCMC* algorithm [23], a generalization that is motivated by genetic algorithms [29]. This extension offers substantial improvement over the previously employed parallel tempering [18] and yielded a sampler that reliably converged toward the true posterior distribution in the examples discussed below. More details on the implementation of the evolutionary MCMC algorithm can be found in section 2.6.

2.3. Data and signal waveform

Our simulated data consist of simultaneous measurements from several interferometric detectors, superimposed with interferometer-specific Gaussian noise. The signal waveform that was injected into and recovered from the data was implemented using a 3.5 post-Newtonian (PN) approximation for the phase evolution [19, 30] and a 2.5 PN model for the amplitude [21]. The nine parameters determining the responses at different interferometers are: individual masses ($m_1, m_2 \in \mathbb{R}^+; m_1 \leqslant m_2$), luminosity distance ($d_L \in \mathbb{R}^+$), inclination angle ($\iota \in [0, \pi]$), coalescence phase ($\phi_0 \in [0, 2\pi]$), coalescence time at geocenter ($t_c \in \mathbb{R}$), declination $\left(\delta \in \left[-\frac{\pi}{2}, \frac{\pi}{2}\right]\right)$, right ascension ($\alpha \in [0, 2\pi]$) and polarization angle ($\psi \in [0, \pi]$). In order to derive the waveform at an individual interferometer I, the 'local parameters' altitude ($\vartheta^{(I)}$), azimuth ($\varphi^{(I)}$) local coalescence time $\left(t_c^{(I)}\right)$ and local polarization ($\psi^{(I)}$) need to be determined for each interferometer. More specific definitions are given in [18, 31]. An appropriate way of dealing with the failure of the waveform approximation shortly before coalescence still needs to be found. For now we simply terminate the waveform as soon as the innermost stable orbit [19] is reached or as the (3.5 PN) approximated orbital frequency starts decreasing. The latter usually happens first; it is a non-physical effect that has also been noted in other contexts and gives an indication of the obvious failure of the waveform approximation [32, 33]. In future, numerical integration might be used to extrapolate still further. The same approach could be used with a wide range of waveforms; in previous studies we have used implementations of the 2.0 PN stationary-phase approximation [17], and

a 2.5 PN phase and 2.0 PN amplitude approximation [18]. We are also currently working on an extension to the case of spinning binaries, which entails the consideration of several additional parameters.

2.4. Priors

We applied non-informative priors on the 'geometrical' parameters that describe the inspiral event's location and orientation. Assuming that any direction and orientation is equally likely (or none of these is *a priori* 'preferred'), this leads to uniform priors for right ascension α, polarization angle ψ and coalescence phase ϕ_0, and to prior densities

$$f(\delta) = \tfrac{1}{2}\cos(\delta) \qquad \text{and} \qquad f(\iota) = \tfrac{1}{2}\sin(\iota) \tag{1}$$

for declination δ and inclination angle ι. These also define the *maximum entropy* settings for these parameters [25]. The coalescence time t_c is assumed to be known in advance up to a certain accuracy from the detection pipeline that would in reality precede such an analysis [10]. For our demonstration purposes we set its prior to be uniform across ± 5 ms around the true value (which of course is known for simulated data); using wider ranges only makes the search phase longer, due to the larger parameter space [18]. The prior for the masses (m_1, m_2) reflects the distribution of the masses among binary inspirals, which could be based on observational evidence [34, 35] as well as theoretical considerations [36, 37]. For now, we simply defined it as uniform across a range of 1–10 $\mathrm{M}_\odot$. In principle, this type of search will be applicable for component masses up to 20 $\mathrm{M}_\odot$ (which corresponds to the low frequency sensitivity limit for LIGO and Virgo).

Assuming that inspirals happen uniformly across space leads to a prior $\mathrm{P}(d_L \leqslant x) \propto x^3$ for the luminosity distance d_L. This is an improper prior, seemingly implying there was an 'infinite' probability for 'infinitely remote' inspiral events. It is also unrealistic, since an inspiral event needs to happen within a certain range in order to be detectable, otherwise its signal would be too faint to be noted at all. We incorporated this restriction into the prior specification by considering the *detection probability* of an inspiral event, depending on the signal-to-noise ratio (SNR). A signal's SNR increases linearly with its amplitude, so for the prior definition we use the amplitude as an approximation to the SNR. Further simplifying its expression (and considering only the intrinsic parameters' effects on the amplitude) we define

$$\begin{aligned}\mathcal{A}(m_1, m_2, d_L, \iota) &:= \ln\left(\frac{\sqrt{\eta}\, m_t^{\frac{5}{6}}}{d_L}\right) + \ln\left(\underbrace{\sqrt{(1+\cos(\iota)^2)^2 + (2\cos(\iota))^2}}_{\geqslant 1 \text{ and } \leqslant\sqrt{8}\,\approx 2.8}\right) \\ &= \ln\left(\frac{\sqrt{\eta}\, m_t^{\frac{5}{6}}}{d_L}\right) + \frac{1}{2}\ln\left(1 + 6\cos^2\iota + \cos^4\iota\right), \end{aligned} \tag{2}$$

where $m_t = m_1 + m_2$ is the *total mass* and $\eta = \frac{m_1 m_2}{m_t^2}$ is the *(symmetric) mass ratio* of the inspiralling system ($\mathcal{A}$ is actually proportional to the *logarithmic* amplitude) [17]. Now one could set a threshold amplitude below which the corresponding event would be considered undetectable, but we preferred a smoother transition that does not strictly rule out parts of the parameter space. We do so by modeling the *detection probability*,

$$D_{a,b}(x) = \frac{1}{1 + \exp\left(\frac{x-a}{b}\right)}, \tag{3}$$

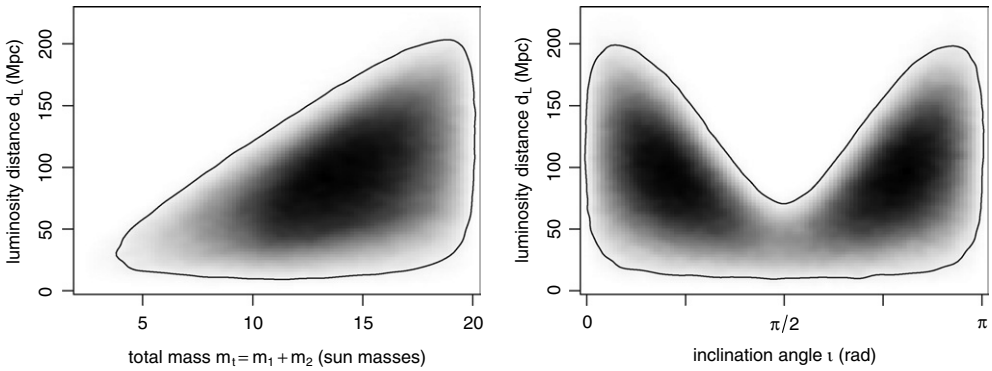

Figure 1. Marginal joint prior densities for total mass m_t and distance d_L, and inclination ι and distance d_L. The contour line encloses a 99% credibility region.

as a (sigmoidal) function of the amplitude value x. The values of a and b are set by defining at which amplitudes x_L and x_U the detection probability reaches some value p and exceeds $1 - p$ (where $0 < p < 0.5$, e.g., $p := 0.1$). Given x_L and x_U, these are set to

$$a := \frac{x_L + x_U}{2} \qquad \text{and} \qquad b := \frac{x_U - x_L}{2 \log\left(\frac{p}{1-p}\right)}. \tag{4}$$

In the following, we defined $p := 0.1$, $x_U := \mathcal{A}(2\ \mathrm{M}_\odot, 2\ \mathrm{M}_\odot, 50\ \mathrm{Mpc}, 0)$ and $x_L := \mathcal{A}(2\ \mathrm{M}_\odot, 2\ \mathrm{M}_\odot, 60\ \mathrm{Mpc}, 0)$, assuming that a 2–2 $\mathrm{M}_\odot$ inspiral with zero inclination is detectable out to distances of 50 and 60 Mpc with 90% and 10% probability, respectively, and providing a reasonable coverage of the parameter space for the example below. More realistic bounds may be specified with respect to a certain detection pipeline that is supposed to be installed upstream. Considerations within a similar context (long-term observations of pulsars' gravitational wave signals) indeed show that while detection of signals is certain for high amplitudes and impossible for low amplitudes, there is also a transition region in-between where detectability is a matter of chance [38, 39]. The detection probability then enters the prior definition as an additional factor. Considering 'occurrence' and 'detection' probabilities this way then leads to a proper prior distribution for all parameters, reflecting the knowledge about the inspiral signal *given* that it released a trigger in the pipeline. Figure 1 illustrates some marginal prior densities resulting from the above settings.

One could actually explicitly use the SNR for the prior instead of approximating it by $\mathcal{A}$. An SNR computation in general is computationally about as expensive as a likelihood evaluation; but once one has done the likelihood evaluation for given parameter values, the SNR computation would simplify, since it could partly build on computations done in the first step. When approximating the SNR by $\mathcal{A}$, any effects of the mass parameters besides their effect on the overall amplitude are neglected, as well as the impact of the antennae patterns, i.e. the sensitivities of the individual interferometers with respect to the signal's sky location.

The above definitions imply that, e.g., greater masses have a greater prior probability (since, resulting in greater amplitudes, they are still detectable at farther distances, see figure 1), although *initially* any masses were assumed to occur equally likely. An analogous effect is known in astronomy as the *Malmquist effect*; incorporating it into the prior definition will compensate for selection bias that would otherwise affect the parameter estimates [40, 41].

2.5. Likelihood

We assume that the noise is independent between different interferometers. Consequently, the likelihood for each site can be computed individually, and the network likelihood then arises as the product of the individual likelihoods. Individual likelihoods are computed based on Fourier transforms of data and signal, and the noise spectrum, which is specific for each interferometer [42]. More details about the likelihood computation are given in [18].

2.6. MCMC implementation

We implemented the MCMC sampler as a basic Metropolis algorithm [16, 27] that first was extended to a parallel tempering algorithm. The 'tempering' here works as in a simulated annealing algorithm [28] and prevents MCMC chains from getting stuck in local modes of the posterior distribution. Parallel tempering then is the special case of a Metropolis-coupled MCMC (MCMCMC) algorithm [16], where several tempered MCMC chains, each at different temperatures, are run in parallel, and additional proposals are introduced to 'swap' parameter sets between chains [18, 43]. This algorithm can be further refined by implementing elements of genetic algorithms [29]. The set of parallel chains may be thought of as constituting a 'population' whose individuals may be crossed to form 'hybrids' that inherit properties from both 'parental' chains, the result being an evolutionary MCMC algorithm [23]. The 'crossovers' between sets of parameters were implemented as *real crossovers*, in which offsprings are formed by randomly reassembling the parental parameter sets, as well as *snooker crossovers*, in which a new offspring is proposed somewhere on the straight line connecting the two parental points in parameter space [44]. Internally, instead of the original mass parameters, the chirp mass $m_c = \frac{(m_1 m_2)^{3/5}}{(m_1+m_2)^{1/5}}$ and the (symmetric) mass ratio $\eta = \frac{m_1 m_2}{(m_1+m_2)^2}$ were used, since these are easier to sample from.

3. Example application

We applied our MCMC routine to a simulated data set, corresponding to an inspiral signal that is received at three interferometers, specifically the two LIGO sites Hanford (LHO) and Livingston (LLO), and the Virgo interferometer near Pisa (V). The simulated inspiral involved masses of $m_1 = 2\ \mathrm{M}_\odot$ and $m_2 = 5\ \mathrm{M}_\odot$ (chirp mass $m_c = 2.70\ \mathrm{M}_\odot$, mass ratio $\eta = 0.204$), observed from a distance of $d_L = 30$ Mpc at $t_c = 700\,009\,012.345$ GPS seconds. For the synthesized data that we use, the noise characteristics were assumed to match the target sensitivities for LIGO and Virgo [45]. The resulting SNRs [18] at the three sites were 8.4 (LHO), 10.9 (LLO), 6.4 (V), and the network SNR was 15.2.

Figure 2 shows the marginal posterior distributions for several individual parameters in comparison to the true values for the injected signal. While some of the (marginal) distributions appear roughly Gaussian, others are clearly not, and some even possess multiple modes. This illustrates some of the strengths of a fully Bayesian approach: no approximations to the posterior's (or likelihood's) shape are made, an irregular posterior surface does not pose a problem, and the assessment of relative importance of multiple modes arises as a matter of course [18]. Figure 3 illustrates the joint distributions of two pairs of parameters. The high correlation between the chirp mass and the mass ratio indicates some degeneracy between these two parameters. Table 1 lists some numerical estimates for individual parameters for our specific example.

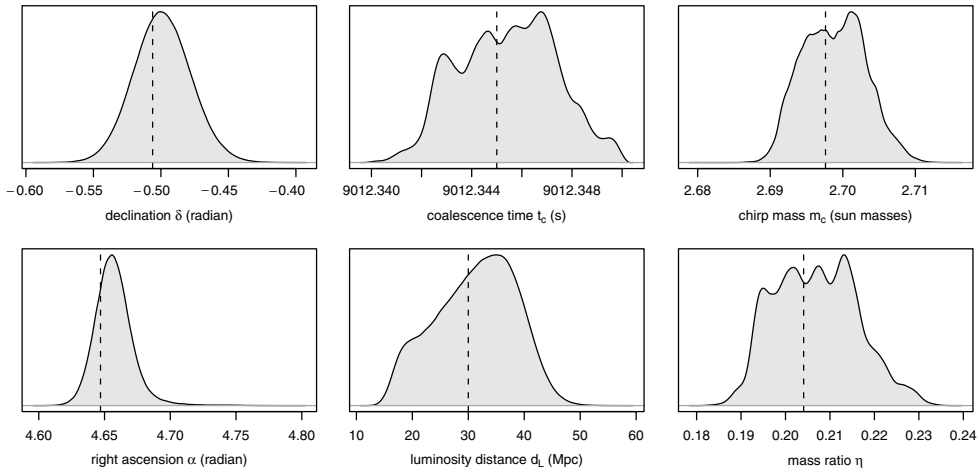

Figure 2. Marginal joint posterior densities for some of the parameters. Dashed lines indicate the true parameter values.

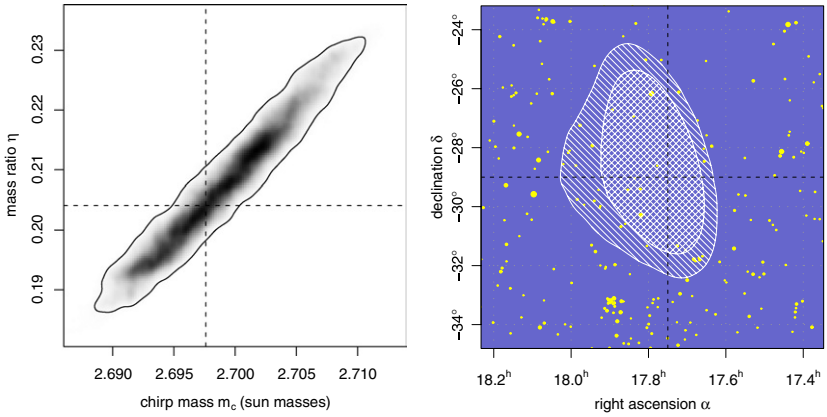

Figure 3. Left: marginal joint posterior density for the two mass parameters, and a 99% credibility region. Right: 95% and 99% credibility regions for the sky location against the backdrop of the night sky. Dashed lines indicate the true values.

(This figure is in colour only in the electronic version)

4. Discussion

We have presented a description of our coherent MCMC code for estimating nine parameters associated with a binary inspiral signal detected by a network of interferometric detectors. This program uses time-domain inspiral templates that are 3.5 PN in phase and 2.5 PN in amplitude. New MCMC techniques, such as evolutionary MCMC and genetic algorithms, have been implemented in our code. The code can be applied to inspiral signals where the masses of the components can be as large as 20 $M_\odot$; inspirals with large mass ratios can also be successfully analyzed. This code is part of a large mass ratio inspiral detection pipeline that we are currently developing; a *loose-net* inspiral detection pipeline (using, for example,

Table 1. Some key figures of the individual parameters' marginal posterior distributions, where meaningful. Mean and standard deviation illustrate location and spread, and the 95% central credible interval gives a range that contains the true parameter with 95% probability, given the data at hand.

	Mean	Standard deviation	95% c.c.i.	True	Unit
Chirp mass (m_c)	2.6988	0.0043	(2.6913, 2.7071)	2.6976	$M_\odot$
Mass ratio (η)	0.2069	0.0092	(0.1917, 0.2258)	0.2041	
Coalescence time (t_c)	12.3454	0.0019	(12.3420, 12.3491)	12.3450	s
Luminosity distance (d_L)	31.3	7.2	(17.4, 43.6)	30.0	Mpc
Inclination angle (ι)	0.737	0.343	(0.160, 1.462)	0.700	rad
Declination (δ)	−0.499[a]	} 0.025[a]	(−0.540, −0.457)	−0.506	rad
Right ascension (α)	4.657[a]		(4.632, 4.689)	4.647	rad
Coalescence phase (ϕ_0)	2.84[a]	1.38[a]		2.0	rad

[a] Mean direction and spherical standard deviation (suitable for angular variables) [46].

lower order PN templates) will generate a reasonable number of triggers, and this MCMC will then be applied to those times where triggers were recorded. The next logical extension of our binary inspiral MCMC work will be to systems with spin. The addition of spin will increase the number of parameters needed for the model, and consequently will increase the complexity and the time required to run the MCMC. This is currently an area of active research for us.

Acknowledgments

This work was supported by the Marsden Fund Council from Government funding, administered by the Royal Society of New Zealand (grant UOA-204), National Science Foundation grant PHY-0553422 and the Fulbright Scholar Program.

References

[1] Abbott B *et al* 2004 Detector description and performance for the first coincidence observations between LIGO and GEO *Nucl. Instrum. Methods Phys. Res.* A **517** 154–79
[2] Sigg D 2004 Commissioning of LIGO detectors *Class. Quantum Grav.* **21** S409–15
[3] Acernese F *et al* 2006 The status of VIRGO *Class. Quantum Grav.* **23** S63–70
[4] Acernese F *et al* 2005 Status of VIRGO *Class. Quantum Grav.* **22** S869–80
[5] Lück H *et al* 2006 The status of GE0600 detector *Class. Quantum Grav.* **23** S71–8
[6] Takahashi R *et al* 2003 Operational status of TAMA300 *Class. Quantum Grav.* **20** S593–8
[7] Taylor J H and Weisberg J M 1989 Further experimental tests of relativistic gravity using the binary pulsar PSR1913 + 16 *Astrophys. J.* **345** 434–50
[8] Abbott B *et al* 2004 Analysis of LIGO data for gravitational waves from binary neutron stars *Phys. Rev.* D **69** 122001
[9] Marion F *et al* 2004 Gravitational waves and experimental gravity *Proc. of the Rencontres de Moriond 2003* (Gif-sur-Yvette: Editions Frontiáeres)
[10] Amico P *et al* 2003 A parallel Beowulf-based system for the detection of gravitational waves in interferometric detectors *Comput. Phys. Commun.* **153** 179–89
[11] Beauville F *et al* 2007 Detailed comparison of LIGO and Virgo inspiral pipelines in preparation for a joint search *Preprint* gr-qc/0701027
[12] Abbott B *et al* 2005 Search for gravitational waves from galactic and extra-galactic binary neutron stars *Phys. Rev.* D **72** 082001
[13] Abbott B *et al* 2005 Search for gravitational waves from primordial black hole binary coalescences in the galactic halo *Phys. Rev.* D **72** 082002
[14] Abbott B *et al* 2006 Search for gravitational waves from binary black hole inspirals in LIGO data *Phys. Rev.* D **73** 062001
[15] Abbott B *et al* 2006 Joint LIGO and TAMA300 search for gravitational waves from inspiralling neutron star binaries *Phys. Rev.* D **73** 102002

[16] Gilks W R, Richardson S and Spiegelhalter D J 1996 *Markov chain Monte Carlo in Practice* (Boca Raton, FL: Chapman & Hall/CRC)
[17] Röver C, Meyer R and Christensen N 2006 Bayesian inference on compact binary inspiral gravitational radiation signals in interferometric data *Class. Quantum Grav.* **23** 4895–906
[18] Röver C, Meyer R and Christensen N 2007 Coherent Bayesian inference on compact binary inspirals using a network of interferometric gravitational wave detectors *Phys. Rev.* D **75** 062004
[19] Blanchet L, Faye G, Iyer B R and Joguet B 2002 Gravitational-wave inspiral of compact binary systems to 7/2 post-Newtonian order *Phys. Rev.* D **65** 061501 (note the erratum [20])
[20] Blanchet L, Faye G, Iyer B R and Joguet B 2005 Gravitational-wave inspiral of compact binary systems to 7/2 post-Newtonian order *Phys. Rev.* D **71** 129902 (erratum) (see also [19])
[21] Arun K G, Blanchet L, Iyer B R and Qusailah M S S 2004 The 2.5 PN gravitational wave polarizations from inspiralling compact binaries in circular orbits *Class. Quantum Grav.* **21** 3771–801 (note the erratum [22])
[22] Arun K G, Blanchet L, Iyer B R and Qusailah M S S 2005 The 2.5 PN gravitational wave polarizations from inspiralling compact binaries in circular orbits *Class. Quantum Grav.* **22** 3115–7 (corrigendum) (see also [21])
[23] Liang F and Wong H W 2001 Real-parameter evolutionary Monte Carlo with applications to Bayesian mixture models *J. Am. Stat. Assoc.* **96** 653–66
[24] Finn L S 1997 Issues in gravitational wave data analysis *Preprint* gr-qc/9709077
[25] Jaynes E T 2003 *Probability Theory: The Logic of Science* (Cambridge: Cambridge University Press)
[26] Gregory P C 2005 *Bayesian Logical Data Analysis for the Physical Sciences* (Cambridge: Cambridge University Press)
[27] Gelman A, Carlin J B, Stern H and Rubin D B 1997 *Bayesian Data Analysis* (Boca Raton, FL: Chapman & Hall/CRC)
[28] Press W H, Teukolsky S A, Vetterling W T and Flannery B P 1992 *Numerical Recipes in C: The Art of Scientific Computing* 2nd edn (Cambridge: Cambridge University Press)
[29] Goldberg D E 1989 *Genetic Algorithms in Search, Optimization, and Machine Learning* (Reading, MA: Addison-Wesley)
[30] Blanchet L, Damour T, Esposito-Farèse G and Iyer B R 2004 Gravitational radiation from inspiralling compact binaries completed at the third post-Newtonian order *Phys. Rev. Lett.* **93** 091101
[31] Blanchet L 2001 Post-Newtonian computation of binary inspiral waveforms *Gravitational Waves: Proc. of the Como School on Gravitational Waves in Astrophysics* ed I Ciufolini, V Gorini, U Moschella and P Fré (Bristol: Institute of Physics Publishing) (*Preprint* gr-qc/0104084)
[32] Buonanno A, Cook G B and Pretorius F 2006 Inspiral, merger and ring-down of equal-mass black-hole binaries *Preprint* gr-qc/0610122
[33] Baker J G, van Meter J R, McWilliams S T, Centrella J and Kelly B J 2006 Consistency of post-Newtonian waveforms with numerical relativity *Preprint* gr-qc/0612024
[34] Finn L S 1994 Observational constraints on the neutron star mass distribution *Phys. Rev. Lett.* **73** 1878–81
[35] van Kerkwijk M H, van Paradijs J and Zuiderwijk E J 1995 On the masses of neutron stars *Astron. Astrophys.* **303** 497–501
[36] Belczynski K, Kalogera V and Bulik T 2002 A comprehensive study of binary compact objects as gravitational wave sources: evolutionary channels, rates, and physical properties *Astrophys. J.* **572** 407–31
[37] Janka H-T 2004 Neutron star formation and birth properties *Preprint* astro-ph/0402200
[38] Umstätter R 2006 Bayesian strategies for gravitational radiation data analysis *PhD Thesis*, The University of Auckland (http://hdl.handle.net/2292/377)
[39] Umstätter R *et al* 2007 Setting upper limits from LIGO on gravitational waves from SN1987a *Preprint*, in preparation
[40] Teerikorpi P 1997 Observational selection bias affecting the determination of the extragalactic distance scale *Annu. Rev. Astron. Astrophys.* **35** 101–36
[41] Hendry M A and Simmons J F L 1995 Distance estimation in cosmology *Vistas Astron.* **39** 297–314
[42] Finn L S and Chernoff D F 1993 Observing binary inspiral in gravitational radiation: one interferometer *Phys. Rev.* D **47** 2198–219
[43] Hukushima K and Nemoto K 1996 Exchange Monte Carlo method and application to spin glass simulations *J. Phys. Soc. Japan* **65** 1604–8
[44] Gilks W R, Roberts G O and George E I 1994 Adaptive direction sampling *Statistician* **43** 179–89
[45] Beauville F *et al* 2005 A first comparison between LIGO and Virgo inspiral search pipelines *Class. Quantum Grav.* **22** S1149–58
[46] Mardia K V and Jupp P E 2000 *Directional Statistics* (Chichester: Wiley)